3GPP TSG RAN WG1 Meeting #86bis **R1-167106**
Göteborg, Sweden, 22nd - 26th Aug 2016

Source: **CMCC**
Title: **Phase Noise Measurement/Modeling and LLS for High Frequency Numerology**
Agenda Item: **8.1.3.1**
Document for: **Discussion and Decision**

1. Introduction

The increasing problem of limited bandwidth and congestion in currently used frequency bands (sub 6GHz) has become a significant limitation for wireless communication systems in recent years. In [1], it is agreed that the new radio access technology (RAT) will consider frequency ranges up to 100GHz. For high frequency spectrum above 6GHz, RF impairments such as phase noise (PN), I/Q imbalance and PA non-linearity will be limiting factors for the performance of high frequency systems. In this contribution we mainly address phase noise, which is caused by imperfect oscillator, in the context of the new RAT with a focus on above-6GHz scenarios where phase noise induces much more difficult than in sub-6GHz scenarios.

In RAN1#85 meeting, the following agreement on phase noise is achieved (R1-165685):

- The PN modeling in TRP is FFS.
- Realistic PN model should consider total oscillator PSD including the impact of reference clock, loop filter noise and VCO sub-components. (e.g. PLL-based model, multi-pole/zero model)
- Each company should provide the model and the parameters used for the evaluation.
- Companies are encouraged to provide link level evaluation result with the phase noise model.

Furthermore, it is agreed that in UL MIMO the following design considering phase noise should be investigated (R1-165808):

- UL reference signal (RS) design considering phase noise compensation.

Although several PN models have been proposed in R1-165685, it is agreed that other PN model is not precluded. In this contribution, a PN model in TRP based on realistic measurement is proposed and then compared with PN models provided in R1-165685. Next, several considerations on RS design principle for PN compensation are given in this presentation. Finally, extensive link-level simulation (LLS) results based on our proposed PN model are provided. According to the simulation results, several proposals about subcarrier spacing and the number of PN compensation RS per OFDM symbol are given.

2. Phase Noise Measurement/Modeling

■ Proposed phase noise model

According to the PLL phase noise model defined in [2], the PSD of the phase noise can be expressed by:

$$S_{Total}(f) = \begin{cases} S_{Ref}(f) + S_{PLL}(f), & \text{when } f \le loop\ BW \\ S_{VCO_v2}(f) + S_{VCO_v3}(f), & \text{when } f > loop\ BW \end{cases} \quad (1)$$

where

$$S_{Ref/PLL/VCO_v2/VCO_v3} = PSD0 \cdot \left[\frac{1+(f/f_z)^k}{1+f^k}\right] \text{(dB)} \tag{2}$$

$$PSD0 = FOM + 20\log f_c - 10\log\left(\frac{P}{1\,mW}\right) \text{(dB)} \tag{3}$$

In (3), FOM is the figure of merit, f_c is the carrier frequency and P is the consumed power.

This expression (1) is in fact oversimplified based on two assumptions. 1). The first assumption is that the sum of $S_{Ref}(f)$ and $S_{PLL}(f)$ at loop bandwidth (Bw) is equal to the sum of $S_{VCO_v2}(f)$ and $S_{VCO_v3}(f)$. Actually the phase noise of VCO at the stop frequency of the loop is much better than that of the reference and PLL chip. So usually there will be a gap between two parts of the lines described by equation (1) and the gap may be about 10-20 dB. 2). The second assumption is that there are no noise gains for Ref and PLL. In fact, the noise gains for Ref and PLL are big enough and therefore cannot be ignored. And for equation (3) the $PSD0$ can be obtained from vendors, so the equation (3) is no longer used in this contribution.

To compensate this mismatch, we make some corrections on (1) as follows:

$$S_{Total}(f) = \left(S_{Ref}(f) + S_{PLL}(f)\right) \cdot W(f) + \left(S_{VCOv2}(f) + S_{VCO_{v3}}(f)\right) \cdot W(f)/G(f) \tag{4}$$

where

$$S_{Ref/PLL/VCO_v2/VCO_v3} = PSD0 \cdot \left[\frac{1+(f/f_z)^k}{1+f^k}\right] \text{(dB)} \tag{5}$$

$W(f)$ represents the closed loop gain of PLL and $G(f)$ is the forward loop gain.

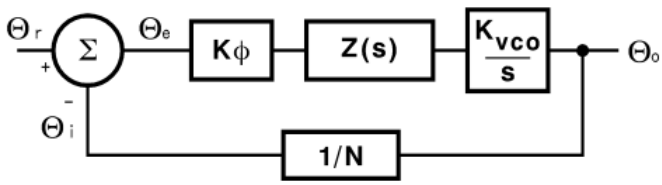

Fig.1. Linear model for PLL loop

The linear model of a PLL is shown in Fig. 1, and according to this model we can define the equations for the phase transfer function as follows:

$$Forward\ loop\ gain = G(s) = \frac{\theta o}{\theta e} = \frac{K\varphi Z(S) Kvco}{S} \tag{6}$$

$$Reverse\ loop\ gain = H(S) = \frac{\theta i}{\theta o} = \frac{1}{N} \tag{7}$$

$$Open\ loop\ gain = H(S)G(S) = \frac{\theta i}{\theta e} = \frac{K\varphi Z(S) Kvco}{NS} \tag{8}$$

$$Closed\ loop\ gain = W(S) = \frac{\theta o}{\theta r} = \frac{G(S)}{1 + H(S)G(S)} \tag{9}$$

where $K\varphi$ is the phase detector/charge pump constant, which represents the phase difference between the

current output and input; $Kvco$ is VCO tuning voltage constant, which represents the tuning ratio of frequency and voltage; N is the main divider ratio, which represents the ratio of carrier frequency and phase detector input frequency; $Z(S)$ is the impedance of the loop filter; $K\varphi$, $Kvco$ and N are constant numbers, which will not affect the shape of $W(S)$ effectively. When the loop filter order, loop Bw and phase margin are set, the shape of the close loop gain is also set, no matter what the values of $K\varphi$, $Kvco$ and N are. N only decides the amplitude of close loop gain, and so is the noise gain of VCO.

■ Model verification

For verification of this model, we check this model with a commercial design. The specification of this design is followed as:

Table 1: Specifications for proposed phase noise models

	BS, Loop Bw = 30kHz			
	REF clk	PLL	VCO V2	VCO V3
Part type	Serdes	HMCXXX	RFVCXXX	
FOM	-275①	-221	-217①	-168①
Fz	1.00E+03, 2.000E+04	4.00E+03	10.00E+06	Inf
k	1,1	0	2	3

① For comparison with other members' proposals, FOM is taken from PSD of datasheet. The calculation method is: $FOM = PSD - 20\log f_c$ (dB)

The configuration of the PLL is as follows:

- Reference frequency: 30.72MHz
- VCO frequency: 15GHz
- Divider ratio N: 488.28125
- 2 order low pass loop filter: loop Bw 30kHz & Phase margin 45degree

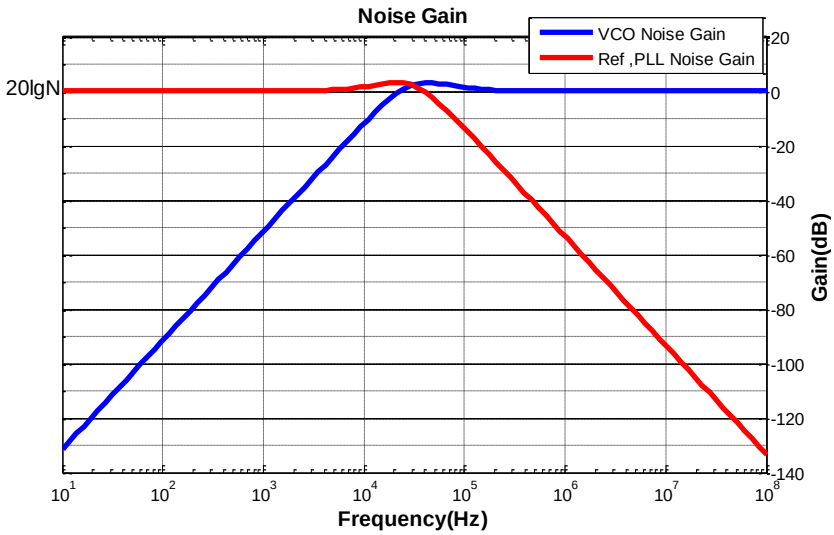

Fig. 2. Noise gain for VCO, PLL and Ref

Fig. 2 describes the noise gain of Ref, PLL and VCO. It can be inferred from this figure that the noise gain for VCO within loop Bw equals to 20lgN. For this configuration, the noise gain is 53.8 dB for Ref and PLL.

Outside of the loop Bw the noise gain performs like a low-pass filter. That means the noise gain for Ref and PLL is reduced by the loop. The noise gain for VCO performs like a high-pass filter without extra amplification of noise.

By using the compensated PN model defined in (4) and the corresponding parameters proposed in Table 1, our proposed PN model is shown in the following Figs 3-5. In Fig. 3, for 15GHz phase noise, we compared our phase model with the realistic BS phase noise measurement (labeled as 'test result'). The result shows that our proposed PN model can match near perfectly. In addition, by observation and calculation, the gap between our proposed model and other models shown in Fig. 3 comes from the noise gain, which is 20lgN in loop bandwidth and should be added in the model as mentioned above. Fig. 4 and Fig. 5 present the comparison of different models in 30GHz and 70GHz, respectively. In summary, we take the noise gain for Ref, PLL and VCO into consideration. By doing so, the PN model can be made more accurate and can therefore represent the real performance of current nowadays' commercial design level.

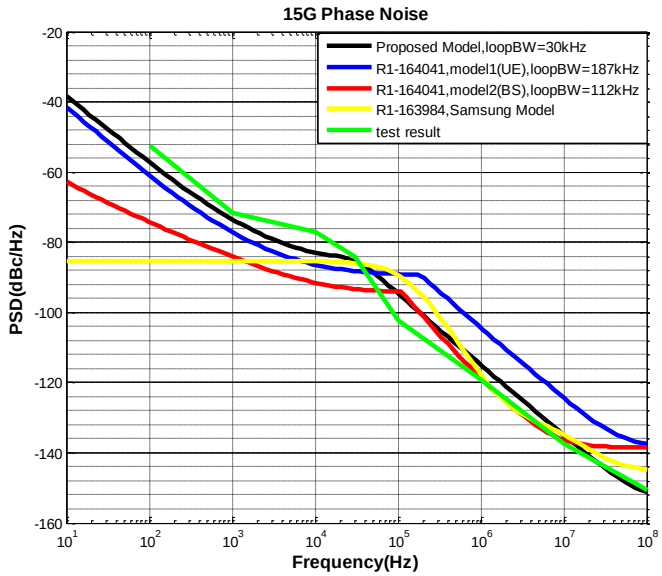

Fig. 3. PSD of our proposed phase noise model (f_c=15GHz)

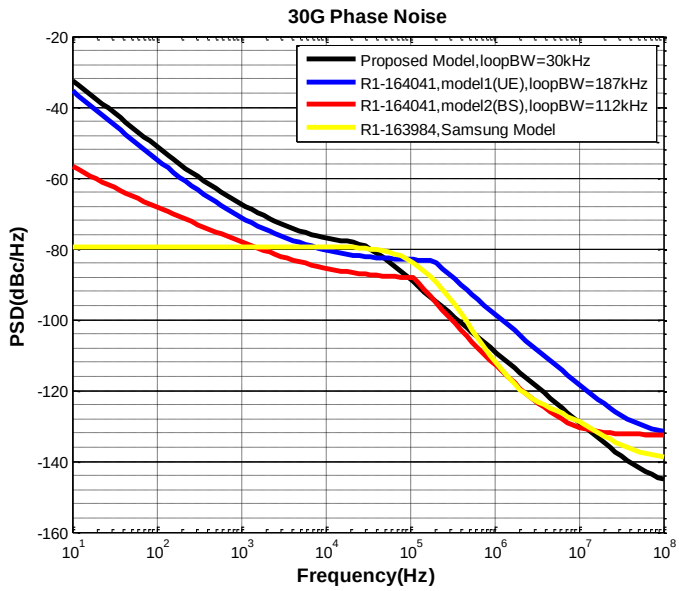

Fig. 4. PSD of our proposed phase noise model (f_c=30GHz)

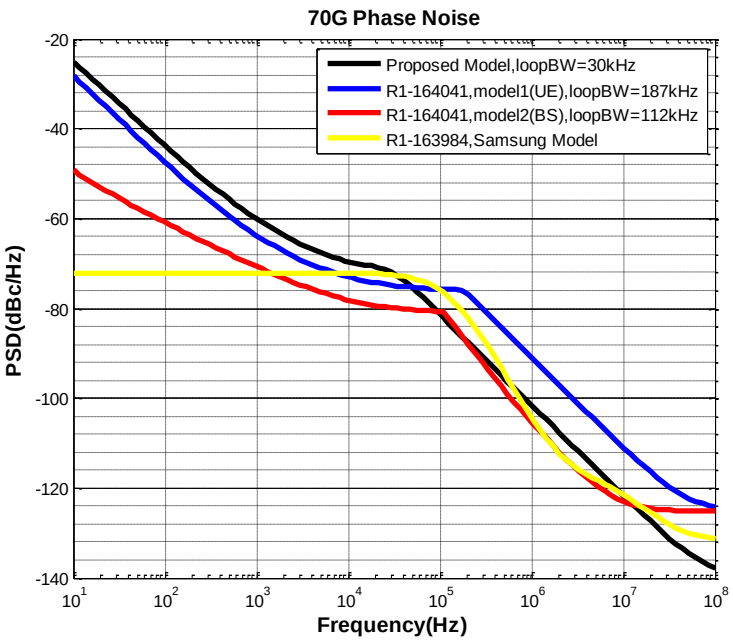

Fig. 5. PSD of our proposed phase noise model (f_c=*70GHz*)

- ***Proposal 1:*** *The noise gain of PLL, Ref and VCO should be considered in phase noise model.*
- ***Proposal 2:*** *The phase noise model proposed by different companies should be compared and corrected with the realistic measurement.*
- ***Proposal 3:*** *The compensated phase noise model described in (4) and Table 1 should be adopted for the design and evaluation of the new radio for above 6GHz.*

3. Consideration on RS Design for Phase Noise Compensation

Considering the fact that the PN changes randomly from one OFDM symbol to another [3], the basic RS design principle for PN compensation is to put PN estimation RS (hereafter referred as PN-specific RS) on each transmitted OFDM symbol in order to track the fast-changing PN, for both UL and DL.

The effect of PN on OFDM-based systems is its induced common phase error (CPE) and inter-carrier interference (ICI) [4]. For PN-induced ICI, usually its estimation and compensation involves matrix inversion and decision feedback [4] [5], which severely complicate the implementation, especially for the UE side. Therefore, the purpose of PN-specific RS is primarily for the estimation of PN-induced CPE (although PN-specific RS can be also used to further estimate ICI if the capability of hardware is satisfied, its detail is not discussed here for practical consideration).

For PN-induced CPE, ideally it can be estimated by using only one PN-specific RS in each OFDM symbol for the reason that it is a rotation that is identical for all subcarriers in one OFDM symbol. However as will be shown in the next section that for practical working SNR ranges, several PN-specific RS within one OFDM symbol must be provided to generate an averaged version of CPE so as to guarantee the performance. In summary, the following PN-specific RS pattern is preferred for high frequency systems:

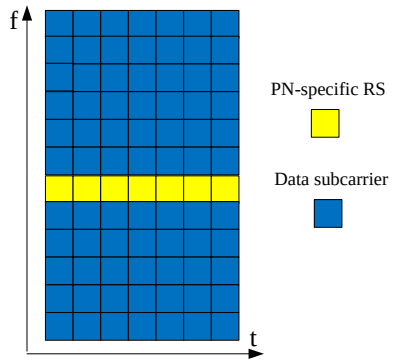

Fig. 6. Proposed PN-specific RS pattern

In Fig.6, the number of PN-specific RS per OFDM symbol is FFS and in the next section, a proposal about the ratio between PN-specific RS and data subcarriers within one OFDM symbol will be given. For multi-user or multi-antenna systems, especially for the UL system, the basic principle for PN-specific RS is to provide orthogonality between different users or different antennas in order to distinguish different users or antennas. For example, if orthogonality is created by orthogonal code (code division multiplexing), then for two UL users the PN-specific RS is shown in Fig. 7. Frequency division multiplexing also applies here and other orthogonal methods between different users or different antennas are FFS.

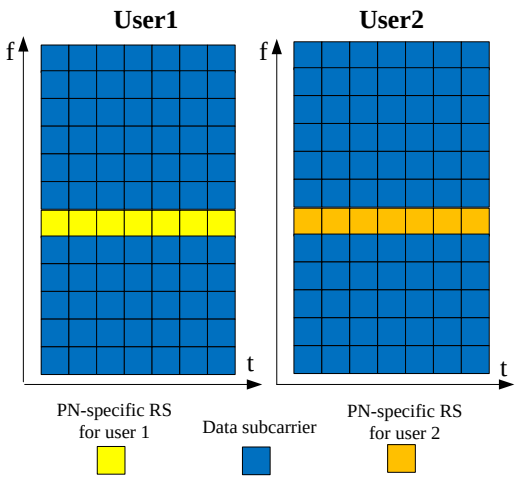

Fig. 7. An example for PN-specific RS pattern of two users, where the orthogonality is created by orthogonal code (different colors are adopted to distinguish PN-specific RS for the two users)

- ***Proposal 4:*** *The basic design principle for PN-specific RS should follow the idea presented in Fig. 6, namely that PN-specific RS should present on every OFDM symbol.*

- ***Proposal 5:*** *For multi-user or multi-antenna systems, the basic design principle for PN-specific RS is to provide orthogonality (by using code division multiplexing, frequency division multiplexing or other orthogonal methods) between different users or different antennas in order to distinguish different users or antennas.*

4. LLS for High Frequency PN

In this section, extensive link-level simulation results are presented to evaluate the effect of PN on high frequency systems. The simulation setting is given in Table 2. To investigate the effect of PN-specific RS number on system performance as mentioned in section 3, equally-spaced PN-specific RS is inserted in each OFDM symbol as exemplified in Fig.6. Furthermore, in order to only analyze the effect of PN on high frequency system, AWGN channel is adopted.

Table 2: Simulation Parameters

Carrier frequency	30GHz, 70GHz
Phase noise model	Proposed PN model in Section 1
Phase noise compensation scheme	Only compensate CPE
Waveform	OFDM
TX/RX number	1 TX/1 RX
FFT size	2048
RB	100
Modulation order	QPSK, 16QAM, 64QAM
Subcarrier spacing	15KHz, 30KHz, 60KHz, 240KHz
Number of PN-specific RS in one OFDM symbol (Corresponding ratio between PN-specific RS and data subcarrier per OFDM symbol)	1 (8.3e-4), 2 (1.7e-3), 5 (4.2e-3), 10 (8.3e-3), 20 (1.67e-2), 50 (4.17e-2), 100 (8.3e-2)
Channel coding	Turbo, 1/3 rate
Channel model	AWGN

■ **<u>30GHz case</u>**:

Fig. 8 presents QPSK BLER vs SNR results with different PN-specific RS number as well as different subcarrier spacing in 30GHz scenario. As can be seen from Fig. 8 that even when low-order modulation scheme QPSK is adopted, the BLER is always equal to 1 if the effect of PN is not compensated (labeled as 'No PN compensation') no matter what the subcarrier spacing is. This demonstrates the detrimental effect of PN on high frequency system and the absolute necessity of cancelling PN. Fig. 8 also shows that as the number of PN-specific RS used to estimate CPE increases, the performance increases as well. When the number is 100, the performance is very close to the ideal case (only about 0.1dB) which assumes no PN (labeled as 'No PN'). When the number is 50, the performance is also very close to the ideal case (only about 0.15dB), but the overhead can be decreased by 50%. Finally, it can be seen from the right-hand side of Fig. 8 that in this case the difference among different subcarrier spacing is negligible.

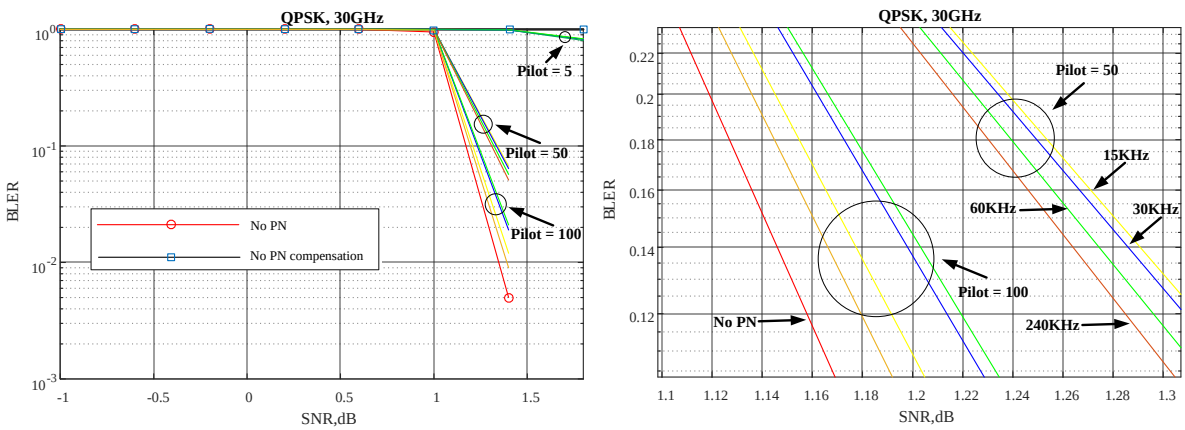

Fig. 8. QPSK BLER vs SNR results with different PN-specific RS number as well as different subcarrier spacing in 30GHz scenario

Fig. 9 presents QPSK MSE vs SNR results with different PN-specific RS number as well as different subcarrier spacing in 30GHz scenario. As can be seen from Fig. 9, as the number of PN-specific RS used to estimate CPE increases, the estimation accuracy increases as well.

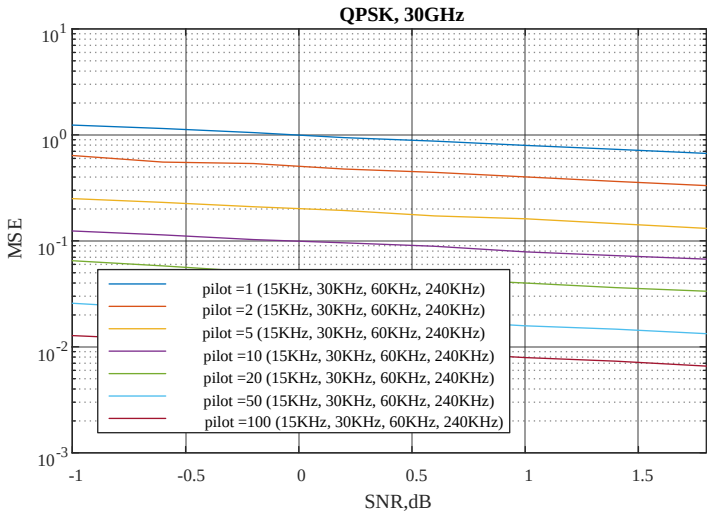

Fig. 9. QPSK MSE vs SNR results with different PN-specific RS number as well as different subcarrier spacing in 30GHz scenario

Fig. 10 presents 16QAM BLER vs SNR results with different PN-specific RS number as well as different subcarrier spacing in 30GHz scenario. The results are similar to those of QPSK case shown in Fig. 8, except that the performance gap between 240KHz and 15KHz subcarrier spacing is slightly larger than that of QPSK case. This shows that as modulation order increases, PN-induced ICI begins to show its effect. The effect of PN-induced ICI can be alleviated by increasing subcarrier spacing as shown in Fig. 10.

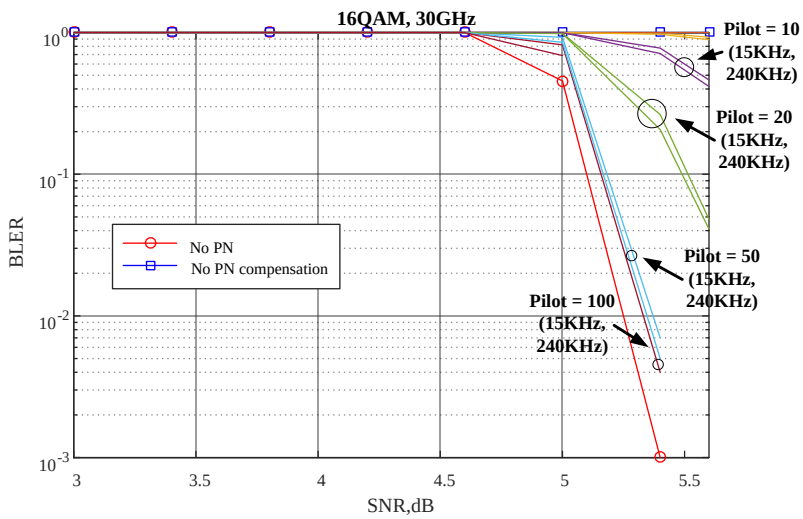

Fig. 10. 16QAM BLER vs SNR results with different PN-specific RS number as well as different subcarrier spacing in 30GHz scenario

Finally, Fig. 11 presents 64QAM BLER vs SNR results with different PN-specific RS number as well as different subcarrier spacing in 30GHz scenario. Compare Fig. 11 with Figs. 9 and 10, it can be seen that the

higher the modulation order becomes, the more obvious that larger subcarrier spacing helps improving the performance. In fact, the phase noise level is the same for these three cases, and therefore the level that the fuzzy or blur the PN-induced ICI to each constellation point is the same on a fixed subcarrier spacing. The performance difference is due to the lower Euclidean distance among constellation points when modulation order goes higher, and therefore its lower PN-induced ICI tolerance. In summary, considering the fact that the larger the subcarrier spacing becomes, the lower the PN-induced ICI becomes, and therefore the better the performance when the modulation order goes higher.

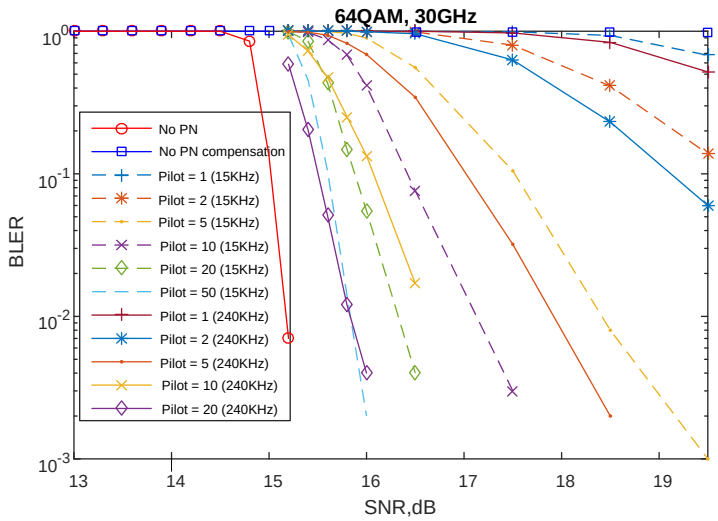

Fig. 11. 64QAM BLER vs SNR results with different PN-specific RS number as well as different subcarrier spacing in 30GHz scenario

- ***Observation 1:*** *At 30GHz, for QPSK and 16QAM modulation schemes, 15KHz subcarrier spacing is in fact enough to guarantee good performance under the condition that enough PN-specific RS is adopted to compensate PN-induced CPE. However as modulation order goes higher, larger subcarrier spacing such as 60KHz or 240KHz should be supported to improve performance. At 30GHz, there is about 0.5dB gain between 240KHz subcarrier spacing and 15KHz subcarrier spacing when modulation order is 64QAM, and the gain is expected to be larger when modulation order goes higher.*

- ***Proposal 6:*** *Up to 240KHz subcarrier spacing should be supported at 30GHz carrier frequency in order to support modulation order higher than 64QAM.*

■ **<u>70GHz case</u>**:

Compare Fig. 4 and Fig. 5, it can be seen that the PN in 70GHz case is even worse than that of 30GHz case (about 15 dBc worse). Fig. 12 shows QPSK BLER vs SNR results with different PN-specific RS number as well as different subcarrier spacing in 70GHz scenario. It can be seen that the PN-induced ICI dominates the effect of PN: when subcarrier spacing is 15 KHz, no matter how many PN-specific RS is used to estimate CPE, there is nearly no performance improvement and error floor occurs. The effect of PN-induced ICI decreases as subcarrier spacing increases. Therefore as can be seen from Fig. 12, the performance is acceptable only when subcarrier spacing is larger than 60KHz (for example the performance of 240 KHz subcarrier spacing is very close to that of the ideal case given that the number of PN-specific RS is 50 or 100).

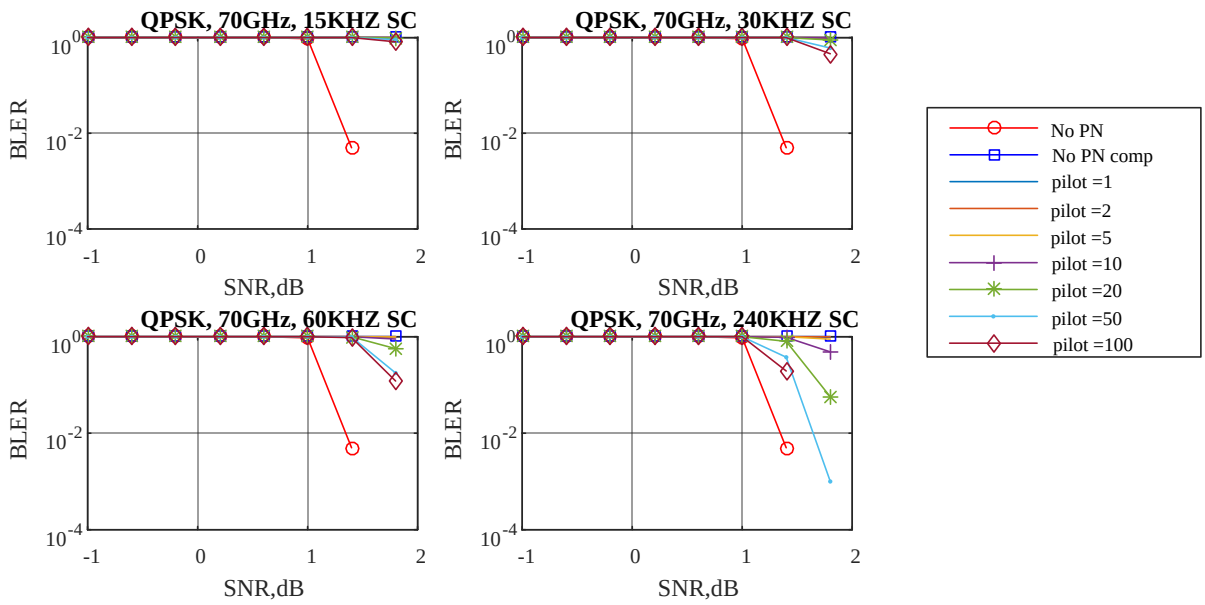

Fig. 12. QPSK BLER vs SNR results with different PN-specific RS number as well as different subcarrier spacing (SC) in 70GHz scenario

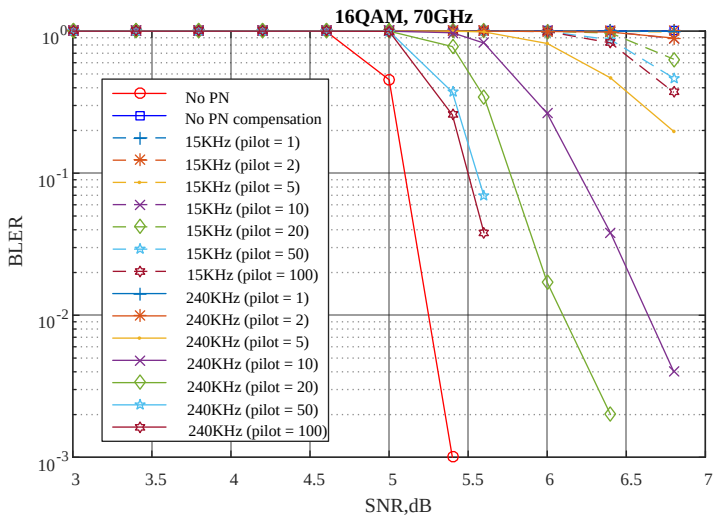

Fig. 13. 16QAM BLER vs SNR results with different PN-specific RS number as well as different subcarrier spacing in 70GHz scenario

Fig. 13 shows 16QAM BLER vs SNR results with different PN-specific RS number as well as different subcarrier spacing in 70GHz scenario. The performance difference between 240KHz and 15KHz is very obvious in this case. This again demonstrates that when carrier frequency goes higher, larger subcarrier spacing must be provided to alleviate the severe PN-induced ICI.

Finally, Fig. 14 shows 64QAM BLER vs SNR results with different PN-specific RS number as well as different subcarrier spacing in 70GHz scenario. This figure shows that even when subcarrier spacing is as large as 240KHz, error floor also occurs. From Fig. 14 it can be implied that either larger subcarrier spacing, for example 480KHz and higher ones, or complicated PN-induced ICI cancellation algorithm must be adopted to improve performance in this scenario.

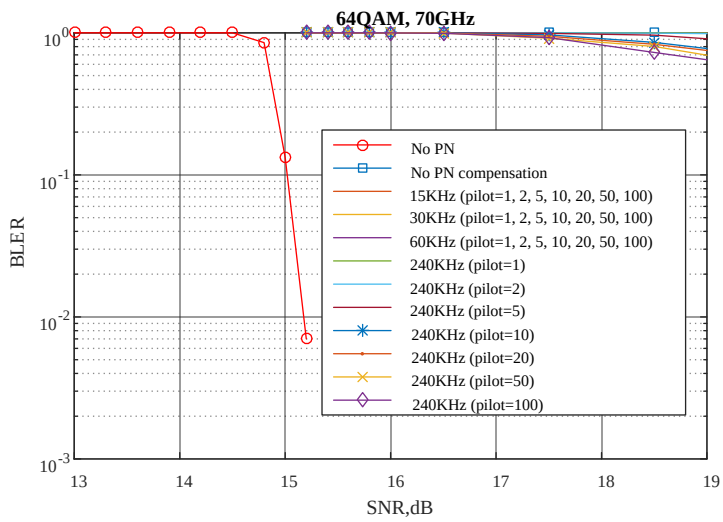

Fig. 14. 64QAM BLER vs SNR results with different PN-specific RS number as well as different subcarrier spacing in 70GHz scenario

- ***Observation 2:*** *As can be seen from the above simulation results, the performance of using only one PN-specific RS per OFDM symbol is far from that of the ideal one, i.e., no PN case.*
- ***Observation 3:*** *When the number of PN-specific RS equals to 50 (4.17e-2), its performance is very close to that of the ideal case, i.e., on PN case.*
- ***Proposal 7*****:** *Multiple PN-specific RS per OFDM symbol should be provided, and the ratio between PN-specific RS and data subcarriers within one OFDM symbol should be about 4% to guarantee good performance.*
- ***Proposal 8:*** *When carrier frequency is 70GHz, subcarrier spacing of 240KHz should be supported in order to maintain good performance up to 16QAM modulation order. And higher subcarrier spacing such as 480KHz or even higher should be supported when modulation order is 64QAM or higher.*

5. Conclusions

In this contribution, CMCC's proposed PN model based on realistic measurement is presented and extensive simulation results based on our proposed PN model are given. The following observations and proposals are achieved:

- ***Proposal 1:*** *The noise gain of PLL, Ref and VCO should be considered in phase noise model.*
- ***Proposal 2:*** *The phase noise model proposed by different companies should be compared and corrected with the realistic measurement.*
- ***Proposal 3:*** *The compensated phase noise model described in (4) and Table 1 should be adopted for the design and evaluation of the new radio for above 6GHz.*
- ***Proposal 4:*** *The basic design principle for PN-specific RS should follow the idea presented in Fig. 6, namely that PN-specific RS should present on every OFDM symbol.*

- ***Proposal 5:*** *For multi-user or multi-antenna systems, the basic design principle for PN-specific RS is to provide orthogonality (by using code division multiplexing, frequency division multiplexing or other orthogonal methods) between different users or different antennas in order to distinguish different users or antennas.*
- ***Observation 1:*** *At 30GHz, for QPSK and 16QAM modulation schemes, 15KHz subcarrier spacing is in fact enough to guarantee good performance under the condition that enough PN-specific RS is adopted to compensate PN-induced CPE. However as modulation order goes higher, larger subcarrier spacing such as 60KHz or 240KHz should be supported to improve performance. At 30GHz, there is about 0.5dB gain between 240KHz subcarrier spacing and 15KHz subcarrier spacing when modulation order is 64QAM, and the gain is expected to be larger when modulation order goes higher.*
- ***Proposal 6:*** *Up to 240KHz subcarrier spacing should be supported at 30GHz carrier frequency in order to support modulation order higher than 64QAM.*
- ***Observation 2:*** *As can be seen from the above simulation results, the performance of using only one PN-specific RS per OFDM symbol is far from that of the ideal one, i.e., no PN case.*
- ***Observation 3:*** *When the number of PN-specific RS equals to 50 (4.17e-2), its performance is very close to that of the ideal case, i.e., on PN case.*
- ***Proposal 7*****:** *Multiple PN-specific RS per OFDM symbol should be provided, and the ratio between PN-specific RS and data subcarriers within one OFDM symbol should be about 4% to guarantee good performance.*
- ***Proposal 8:*** *When carrier frequency is 70GHz, subcarrier spacing of 240KHz should be supported in order to maintain good performance up to 16QAM modulation order. And higher subcarrier spacing such as 480KHz or even higher should be supported when modulation order is 64QAM or higher.*

---

6. References

[1] 3GPP, RP-160671, "New SID Proposal: Study on new radio access technology", NTT DOCOMO, RAN#71, Mar. 2016.

[2] 3GPP, R1-162885, "On the phase noise model for 5G New Radio evaluation", Nokia, Alcatel-Lucent Shanghai Bell, RAN1 #84, Apr. 2016.

[3] Q. Zou *et al.*, "Compensation of phase noise in OFDM wireless systems", IEEE Trans. Signal Process., 55(11), pp. 5407–5424, Nov. 2007.

[4] D. Petrovic *et al.*, "Effects of phase noise on OFDM systems with and without PLL: characterization and compensation", IEEE Trans. Commun., 55(8), pp. 1607–1616, Aug. 2007.

[5] V. Syrjala *et al.*, " Phase noise modelling and mitigation techniques in ODFM communications systems", Wireless Telecommunications Symposium, pp. 1-7, Apr. 2009.